Molecules and Cells

Post-Transcriptional Control of Tropoelastin in Aortic Smooth Muscle Cells Affects Aortic Dissection Onset

You-Fei Qi[1,2], Chang Shu[1,3,*], Zhan-Xiang Xiao[2,*], Ming-Yao Luo[3], Kun Fang[3], Yuan-Yuan Guo[4], Wen-Bo Zhang[2], and Jie Yue[2]

[1]Department of Vascular Surgery, the Second Xiang-ya Hospital, Central South University, Changsha 410011, China, [2]Department of Vascular Surgery, Hainan General Hospital, Haikou 570311, China, [3]Center of Vascular Surgery, Fuwai Hospital, National Center for Cardiovascular Diseases, Chinese Academy of Medical Sciences and Peking Union Medical College, Beijing 100037, China, [4]Department of Vascular Surgery, Fuwai Yunnan Cardiovascular Hospital, Kunming 650032, China
*Correspondence: changshu@vip.126.com (CS); hnxiaozhanxiang@163.com (ZXX)
http://dx.doi.org/10.14348/molcells.2018.2193
www.molcells.org

Aortic dissection (AD) is a catastrophic disease with high mortality and morbidity, characterized with fragmentation of elastin and loss of smooth muscle cells. Although AD has been largely attributable to polymorphisms defect in the elastin-coding gene, tropoelastin (TE), other undermined factors also appear to play roles in AD onset. Here, we investigated the effects of post-transcriptional control of TE by microRNAs (miRNAs) on elastin levels in aortic smooth muscle cells (ASMC). We found that miR-144-3p is a miRNA that targets TE mRNA in both human and mouse. Bioinformatics analyses and dual luciferase reporter assay showed that miR-144-3p inhibited protein translation of TE, through binding to the 3'-UTR of the TE mRNA. Interestingly, higher miR-144-3p levels and lower TE were detected in the ASMC obtained from AD patients, compared to those from non-AD controls. In a mouse model for human AD, infusion of adeno-associated viruses (serotype 6) carrying antisense for miR-144-3p (as-miR-144-3p) under CAG promoter significantly reduced the incidence and severity of AD, seemingly through enhancement of TE levels in ASMC. Thus, our data suggest an essential role of miR-144-3p on the pathogenesis of AD.

Keywords: aortic dissection (AD), aortic smooth muscle cells (ASMC), miR-144-3p, tropoelastin (TE)

INTRODUCTION

Aortic dissection (AD) is a life-threatening condition caused by a tear in the intimal layer of the aorta or bleeding within the aortic wall, resulting in the dissection of aortic wall. More than 70% AD patients would die within 1 week without intervention, while the mortality is still above 20% with medical treatment and surgical intervention (Mallat et al., 2016). Although the exact mechanism underlying AD onset is still uncertain, aortic smooth muscle cells (ASMC), as the main component of aortic media, are believed to be the major affected cells in the formation of AD (Mallat et al., 2016; Morello et al., 2014).

Elastin is a polymeric extracellular protein that determines the extensibility and elastic recoil in many cells, and Elastin in ASMC is more than 50% dry weight of the cells (Morello et al., 2014; Patel and Arora, 2008). Elastin is initially generated as a soluble monomer called tropoelastin (TE) (Patel and Arora, 2008). After TE is secreted, it polymerizes into elastic fibers along with other protein components to form an extracellular elastic matrix, the structure of which determines the mechanical stability and tissue physical properties (Segreto et al., 2014). The human TE gene comprises with 34 exons, resulting in a protein with an alternating arrangement of

Received 9 September, 2017; revised 15 December, 2017; accepted 21 December, 2017; published online 27 February, 2018

eISSN: 0219-1032

hydrophobic and cross-linking domains (Segreto et al., 2014). Although past studies have found that AD may be largely attributable to polymorphisms defect in TE (Isselbacher et al., 2016), other undermined factors, e.g. the TE protein levels and it translational control, may also play roles in AD onset (Sato et al., 2017).

MicroRNAs (miRNAs) are 20~22 nucleotides long non-coding RNAs and are the shortest functional eukaryotic RNAs (Seok et al., 2016). Most of miRNAs attach to the 3′-UTR of genes by imprecisely binding, although there is also a report showing that the binding sites are at the 5′-UTR or extron region (Forman et al., 2008). After binding, genes are silenced because of alternation of spatial structure. MiRNAs play an important role in various biological processes, such as regulation of cell differentiation, cell identity determination, apoptotic cell death, cell migration and cell cycles, et al (Cao et al., 2017; Ivey et al., 2008; Li and Gregory, 2008; Papagiannakopoulos and Kosik, 2009). Among all miRNAs, miR-144 has been extensively studied. Some target genes for miR-144 have been reported, including E26 transformation specific-1 (Zhang et al., 2016), cyclooxygenase-2 (Shao et al., 2016), adenosine triphosphate binding cassette transporter (Vega-Badillo et al., 2016), and cyclin-dependent kinase inhibitor 2D (Jiang et al., 2015). Nevertheless, it is not reported that miR-144 is a targeting miRNA for TE previously.

Here, we investigated the effects of post-transcriptional control of TE by miRNAs on elastin levels in ASMC. We found that miR-144-3p is a miRNA that targets TE mRNA in both human and mouse. Bioinformatics analyses and a dual luciferase reporter assay showed that miR-144-3p inhibited protein translation of TE, through binding to the 3′-UTR of the TE mRNA. Interestingly, higher miR-144-3p levels and lower TE were detected in the ASMC obtained from AD patients, compared to those from non-AD controls. In a mouse model for human AD, infusion of adeno-associated viruses carrying antisense for miR-144-3p (as-miR-144-3p) under CAG promoter significantly reduced the incidence and severity of AD, seemingly through enhancement of TE levels in ASMC.

MATERIALS AND METHODS

Protocol approval

All mouse experiments were approved by and performed according to the guidelines of the Institutional Animal Care and Use Committee of Hainan General Hospital. Female FVB mice of 12 weeks of age (Jackson lab, USA) were kept in specific pathogen free (SPF) conditions, and were used in the current study. Mouse manipulations were performed in accordance with the Principles of Laboratory Care, and supervised by qualified veterinarians. Patient dissection specimens were collected from AD patients who had undergone repair surgery in Hainan General Hospital. None of the patients had aortic diseases that may affect interpretation of the results. Control aortas were obtained from discarded materials from heart transplantation. Informed consent was obtained for use of these specimens form the patients. Use of human tissue was approved by the Medical Ethical Committee of Hainan General Hospital, in accordance with the principles outlined in the Declaration of Helsinki.

Mouse and human ASMC

Human ASMC (HASMC) was purchased from American Type Culture Collection (ATCC, USA; Catalog number: PCS100012), and cultured in vascular Cell Basal Medium (ATCC; Catalog number: PCS100030) plus Vascular Smooth Muscle Cell Growth Kit (ATCC; Catalog number: PCS100042) that contains recombinant human FGFb, insulin, ascorbic acid, L-glutamine, EGF and FBS. Mouse ASMC (MASMC) was isolated from the FVB mice as previously described (Ray et al., 2001). The isolated cells received a negative selection for CD31 by flow cytometry, to remove the contaminated endothelial cells. The phenotype of MASMC was confirmed by expression of both alpha smooth muscle actin (α-SMA) and calponin.

Fluorescence-activated cell sorting (FACS)

Mouse aortic cells were labeled with APC-conjugated CD31 antibody (Becton-Dickinson Biosciences, USA) for negative selection of CD31- cells to get rid of contaminated endothelial cells from the MASMC population. Data were shown with Flowjo software (Flowjo LLC, USA).

RT-qPCR

Total RNA was extracted using an RNeasy kit (Qiagen, Germany). After complementary DNA (cDNA) was generated by reverse transcription, quantitative PCR (RT-qPCR) was performed in duplicates with QuantiTect SYBR Green PCR Kit (Qiagen). All primers were purchased from Qiagen, and the catalog number for the miR-144-3p primer is MS00020328. Data were collected and analyzed using the 2-ΔΔCt method. Values of genes were first normalized against α-tubulin, and then compared to the experimental controls.

Luciferase-reporter activity assay

The target miRNAs for TE in mice and humans was determined by TargetScan, using the context++ score system, as described (Agarwal et al., 2015). The dual-luciferase reporter plasmids, p3′-UTR-TE (containing the wild-type TE 3′-UTR binding site in luciferase reporter plasmid and p3′-UTR-TE-mut (containing the mutant TE 3′-UTR; mut) as well as miR-144-3p, antisense of miR-144-3p (as-miR-144-3p) and a null control were constructed in RiboBio Co. Ltd. (China). For the luciferase assay, the constructed 3′-UTR plasmid and miR-144-3p/as-miR-144-3p were co-transfected into mouse ASMC (MASMC) using Lipofectamine™ 3000 Reagent (Invitrogen, Shanghai China). Then the luciferase activity was detected with the dual-luciferase reporter assay system (Promega, China) after co-transfection cells for 48 hours, following the manufacturer's protocol.

Adeno-associated viruses

The Human Embryonic Kidney 293 cell line (HEK293, ATCC) was used for virus production. We used a pAAV-CAGp-GFP plasmid (Clontech, USA), a packaging plasmid R2C8 carrying the serotype 6 rep and cap genes (Applied Viromics, LLC., USA), and a helper plasmid plAd5 carrying the adenovirus helper functions (Applied Viromics, LLC.) for generating

AAVs in this study. The AAVs were produced by co-transfecting HEK293 cells with the prepared pAAV-CAGp-as-miR-144-3p-2A-GFP or pAAV-CAGp-GFP plasmids, R2C8 and plAd5 by Lipofectamine 3000 (Invitrogen, USA). The viruses were purified using CsCl density centrifugation and then titration was determined by a quantitative densitometric dot-blot assay. These viruses were used to transduce MASMC in vitro using a MOI of 50. For in vivo application, 10^9 viral particles were injected via tail vein of the mice at the beginning of the experiment (first BAPN injection).

Animal model
Female FVB mice of 12 weeks of age were fed with a normal diet and administered freshly prepared β-aminopropionitrile monofumarate (BAPN, Sigma-Aldrich, USA) solution dissolved in the drinking water at a dose of 0.4g BAPN per 100g diet for 6 weeks, as previous described (Sato et al., 2017). Blood pressure was measured using the tail-cuff method. All mice died before the expected end time of the experiment (6 weeks) were autopsied immediately. Mice surviving at the end of the experiment (6 weeks) were sacrificed and their blood and tissue samples were collected for analysis.

Plasma lipid
Plasma levels of triglyceride (TG) and cholesterol (CHO) were measured using COD-PAP and GPO-PAP methods, with respective kits (Abcam, China).

Histology
Histopathological evaluations were performed with samples from control and BAPN-treated mice. Aortas were dissected from the ascending aorta to the iliac artery and were fixed in 10% buffered formalin for 8 hours, as were human tissues. Paraffin-embedded tissues were cut at 5 μm thickness, stained with hematoxylin and eosin following standard procedures.

Western blotting
Proteins were isolated from cultured cells. Primary antibodies were rabbit anti-TE and anti-α-tubulin (Cell Signaling, USA). Secondary antibody is HRP-conjugated anti-rabbit (Dako, USA). Figure images were representative from 5 repeats. α-tubulin was used as a protein loading control.

Statistics
GraphPad prism software (GraphPad Software, Inc., USA) was used for statistical analyses. Unpaired two-tailed Student *t*-test was applied for comparison between two groups. Bivariate correlations were calculated by Spearman's Rank Correlation Coefficients. Data were represented as mean ± SD and were considered significant if $p < 0.05$.

RESULTS

MiR-144-3p is a TE-targeting miRNA highly expressed in mouse and human ASMC
In order to study the post-transcriptional control of TE in ASMC and its relationship with development of AD, we first isolated mouse ASMC (MASMC) from the mouse aorta tissue after a negative selection for CD31 by flow cytometry to

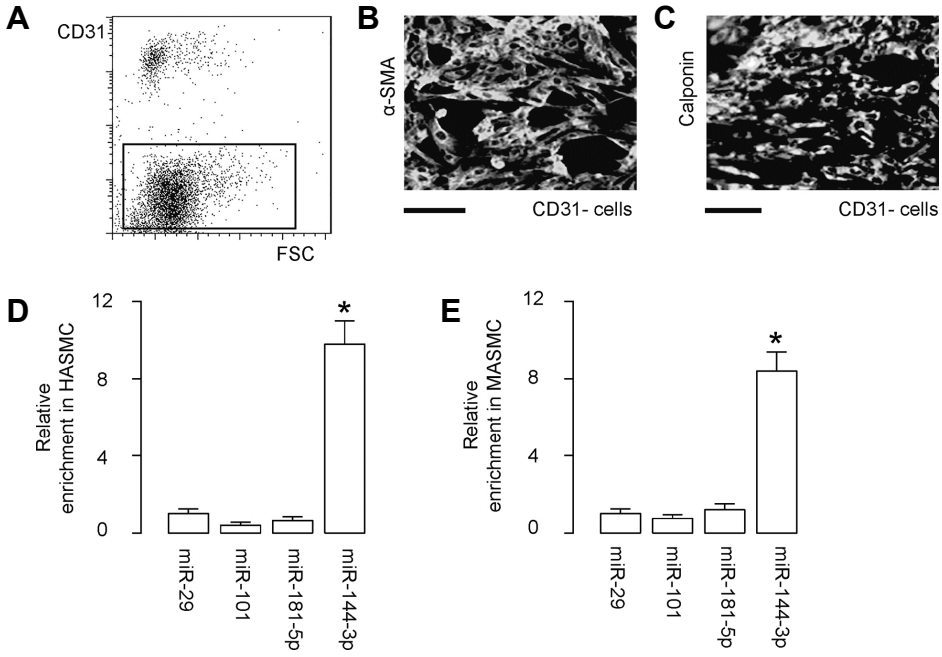

Fig. 1. MiR-144-3p is a TE-targeting miRNA highly expressed in mouse and human ASMC. (A) A representative flow chart for negative selection of mouse aortic cells for CD31 by flow cytometry to remove endothelial cells. (B, C) The purified ASMC (MASMC) was stained for alpha smooth muscle actin (α-SMA; B) and calponin (C). (D, E) Expression of candidate TE-targeting miRNAs (miR-29, miR-101, miR-181-5p and miR-144-3p) in human ASMC (HASMC; D) and in MASMC (E) by RT-qPCR. *$p < 0.05$. NS: non-significant. N = 5.

remove endothelial cells (Fig. 1A). The purified MASMC were stained positive for both alpha smooth muscle actin (α-SMA; Fig. 1B) and calponin (Fig. 1C), confirming the ASMC phenotype. Human ASMC (HASMC) was purchased from ATCC. Next, we used bioinformatics tools to determine the conserved TE-targeting miRNAs in both human and mice, which resulted in 4 candidates, miR-29, miR-101, miR-181-5p and miR-144-3p (Supplementary Table S1). We examined the expression levels of these 4 candidates in ASMC, and found that only miR-144-3p was highly expressed in both HASMC (Fig. 1D) and MASMC (Fig. 1E). Thus, we focused on miR-144-3p in the current study.

MiR-144-3p inhibits protein translation of TE via binding to the 3′-UTR of the TE mRNA

Indeed, bioinformatics revealed that the binding site of miR-144-3p on 3′-UTR of the human TE mRNA is from 856th through 862nd base pair (Fig. 2A), while the binding site of miR-144-3p on 3′-UTR of the mouse TE mRNA is from 833rd through 839th base pair (Fig. 2B). The binding structure on human and mouse is very similar. Thus, our study on this issue using mouse model may be quite translatable to human.

To determine whether the binding of miR-144-3p to TE mRNA indeed inhibits protein translation of TE mRNA, we transfected MASMC with either miR-144-3p or antisense for miR-144-3p (as-miR-144-3p) plasmids. The MASMC were also transfected with a null sequence as a control (null). Alteration of miR-144-3p levels in these miR-144-3p-modified MASMC was validated by RT-qPCR (Fig. 2C). Then, the intact 3′-UTR of wild-type TE mRNA (TE 3′-UTR) and the 3′-UTR of TE mRNA with a mutant at miR-144-3p-binding site (TE 3′-UTR mut) were respectively cloned into luciferase reporter plasmids. MASMC was then co-transfected with one plasmid

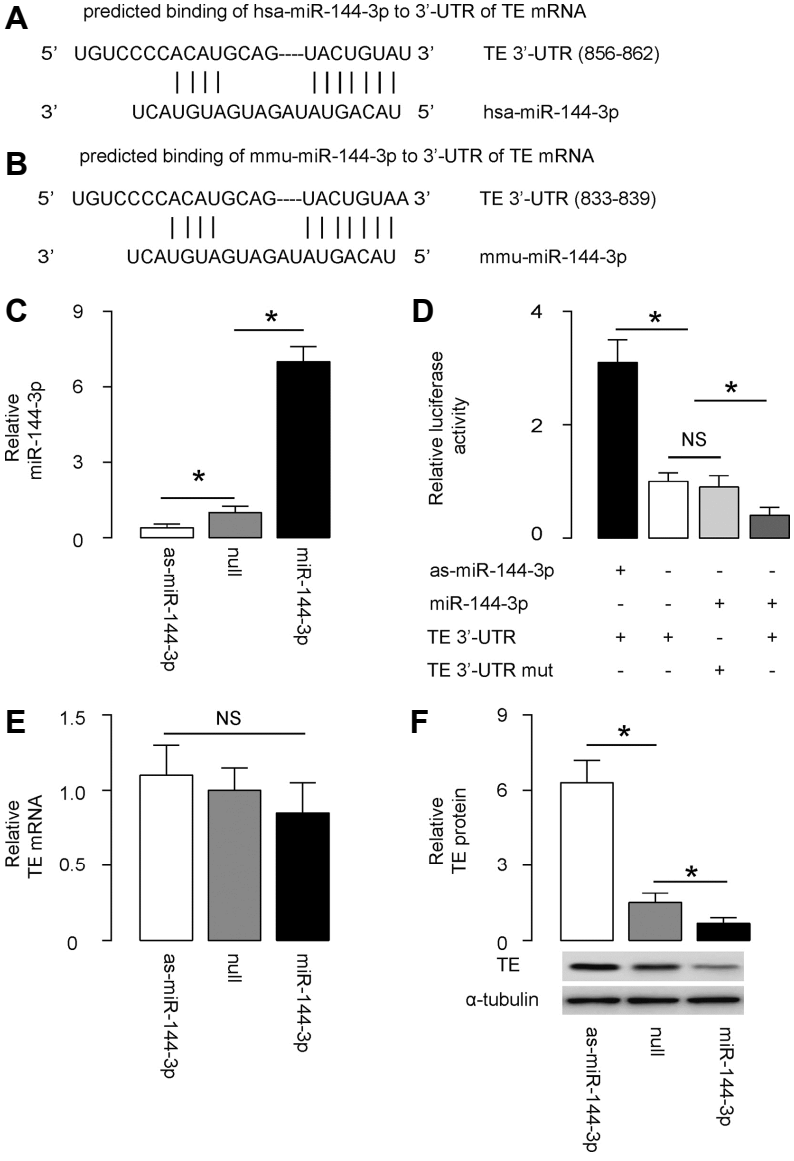

Fig. 2. MiR-144-3p inhibits protein translation of TE via binding to the 3′-UTR of the TE mRNA. (A, B) Bioinformatics revealed that the binding site of miR-144-3p on 3′-UTR of the human TE mRNA is from 856th through 862nd base pair (A), while the binding site of miR-144-3p on 3′-UTR of the mouse TE mRNA is from 833rd through 839th base pair (B). (C) MASMC was transfected with either miR-144-3p or antisense for miR-144-3p (as-miR-144-3p) plasmids. The MASMC were also transfected with a null sequence as a control (null). Alteration of miR-144-3p levels in these miR-144-3p-modified MASMC was validated by RT-qPCR. (D) The intact 3′-UTR of wild-type TE mRNA (TE 3′-UTR) and the 3′-UTR of TE mRNA with a mutant at miR-144-3p-binding site (TE 3′-UTR mut) were respectively cloned into luciferase reporter plasmids. MASMC was then co-transfected with one plasmid from miR-144-3p/as-miR-144-3p/null plasmids and one plasmid from either TE 3′-UTR or TE 3′-UTR mut, and subsequently subjected to a dual luciferase reporter assay. (E-F) RT-qPCR (E) and Western blotting (F) for TE levels in MASMC with adapted miR-144-3p levels. $*p < 0.05$. NS: non-significant. N = 5.

from miR-144-3p/as-miR-144-3p/null plasmids and one plasmid from either TE 3′-UTR or TE 3′-UTR mut, and subsequently subjected to a dual luciferase reporter assay. We found that depletion of miR-144-3p increased the luciferase activity of TE 3′-UTR, while overexpression of miR-144-3p reduced luciferase activity of TE 3′-UTR but had no effect on TE 3′-UTR mut (Fig. 2D). Moreover, alteration of miR-144-3p levels did not alter TE mRNA in MASMC (Fig. 2E), while suppression of miR-144-3p increased TE protein and increases in miR-144-3p inhibited TE protein (Fig. 2F). These results suggested that miR-144-3p specifically targets 3′-UTR of TE mRNA to inhibit its translation in ASMC.

Higher miR-144-3p and lower TE are detected in the ASMC from AD patients

In order to figure out the potential clinical relevance of this miR-144-3p/TE regulatory axis in ASMC for AD onset, we examined the miR-144-3p levels by RT-qPCR and TE levels by Western blotting in obtained ASMC from AD patients, compared to those from non-AD controls. We detected higher miR-144-3p levels (Fig. 3A) and lower TE levels (Fig. 3B) in the ASMC obtained from AD patients, compared to those from non-AD controls. Moreover, the levels of miR-144-3p and TE protein appeared to be inversely correlated (Fig. 3C; $\gamma = -0.72$, $p < 0.0001$, $N = 40$). These data encouraged us to

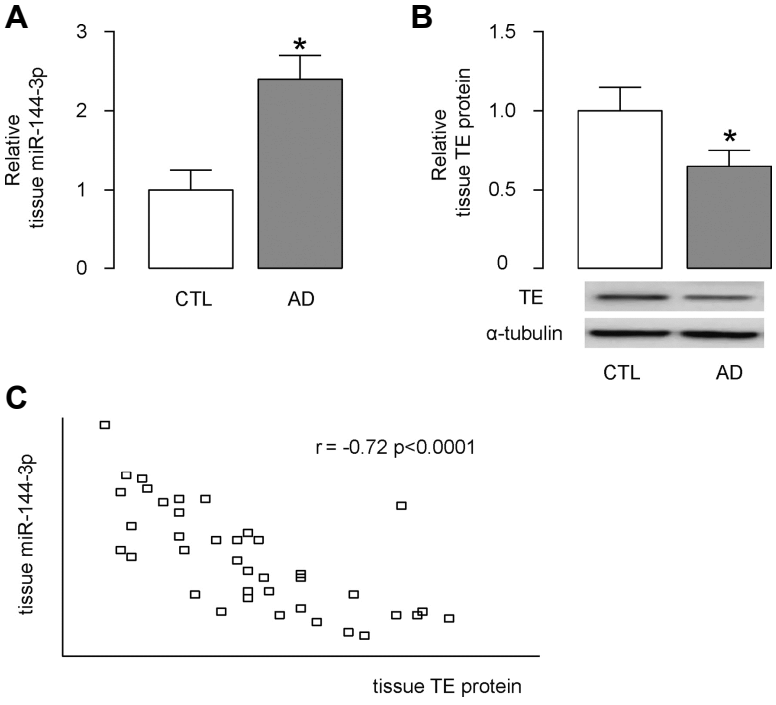

Fig. 3. Higher miR-144-3p and lower TE were detected in the ASMC from AD patients. (A, B) MiR-144-3p levels were examined by RT-qPCR (A) and TE levels were examined by Western blotting (B) in obtained ASMC from AD patients, compared to those from non-AD controls (CTL). (C) A correlation test was performed between miR-144-3p and TE protein, using the 40 specimens.*$p < 0.05$. $N = 40$.

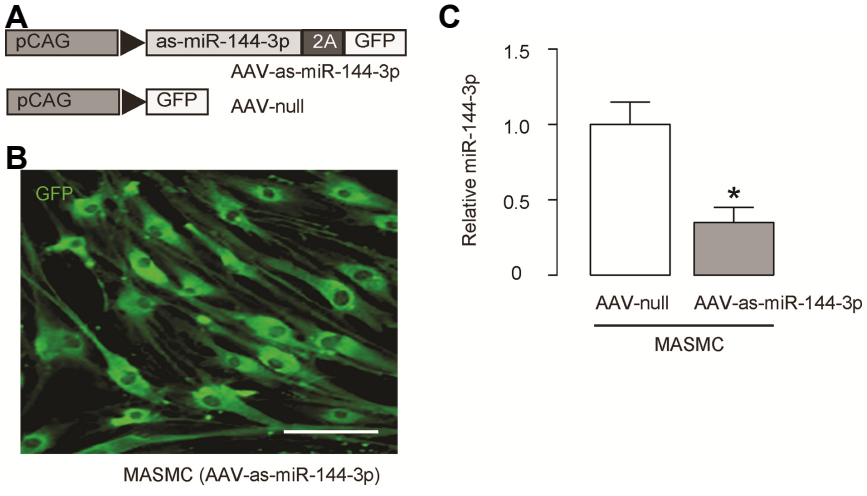

Fig. 4. Preparation of AAV carrying as-miR-144-3p for *in vivo* study. (A) In order to do a loss-of-function experiment in a mouse AD model, we prepared AAV carrying as-miR-144-3p under CAG promoter, and a control AAV. (B) Co-transduction of GFP in the construct allows determination of infection efficiency of MASMC in culture. (C) RT-qPCR for miR-1443p in MASMC transduced with AAV-as-miR-144-3p or control AAV-null viruses. *$p < 0.05$. $N = 5$.

investigate the potential role for AD onset in a mouse model of the involvement of the miR-144-3p/TE regulatory axis in ASMC.

Preparation of AAV carrying as-miR-144-3p for in vivo study

In order to do a loss-of-function experiment in a mouse AD model, we prepared AAV carrying as-miR-144-3p under CAG promoter, and a control AAV (Fig. 4A). Co-transduction of GFP in the construct allows determination of infection efficiency of MASMC in culture (Fig. 4B). We found that the MASMC transduced with AAV-as-miR-144-3p significantly reduced the miR-144-3p levels, compared to in controls (Fig. 4C), suggesting good quality of this AAV.

Suppression of miR-144-3p reduces the incidence and severity of AD

Finally, we performed a mouse model for AD. Ten mice were used in each experimental groups. Three group of mice were included in the study. In group 1, mice did not receive either BAPN or AAVs (CTL). In group 2, mice received BAPN and control AAV-null (BAPN). In group 3, mice received BAPN and AAV-as-miR-144-3p (BAPN+as-miR-144-3p). While no mice developed AD and died in CTL group, 9 from 10 mice in BAPN group developed AD and died within 6 weeks, and only 5 from 10 mice in BAPN group developed AD and died within 6 weeks.

We found that BAPN treatment reduced diastolic blood pressure (Fig. 5A) with no effect on systolic blood pressure (Fig. 5B), indicating increased aortic stiffness. Interestingly, miR-144-3p suppression attenuated the BAPN-induced reduction in diastolic blood pressure (Fig. 5A) without altering systolic blood pressure (Fig. 5B). Moreover, BAPN treatment significantly decreased plasma cholesterol (Fig. 5C)

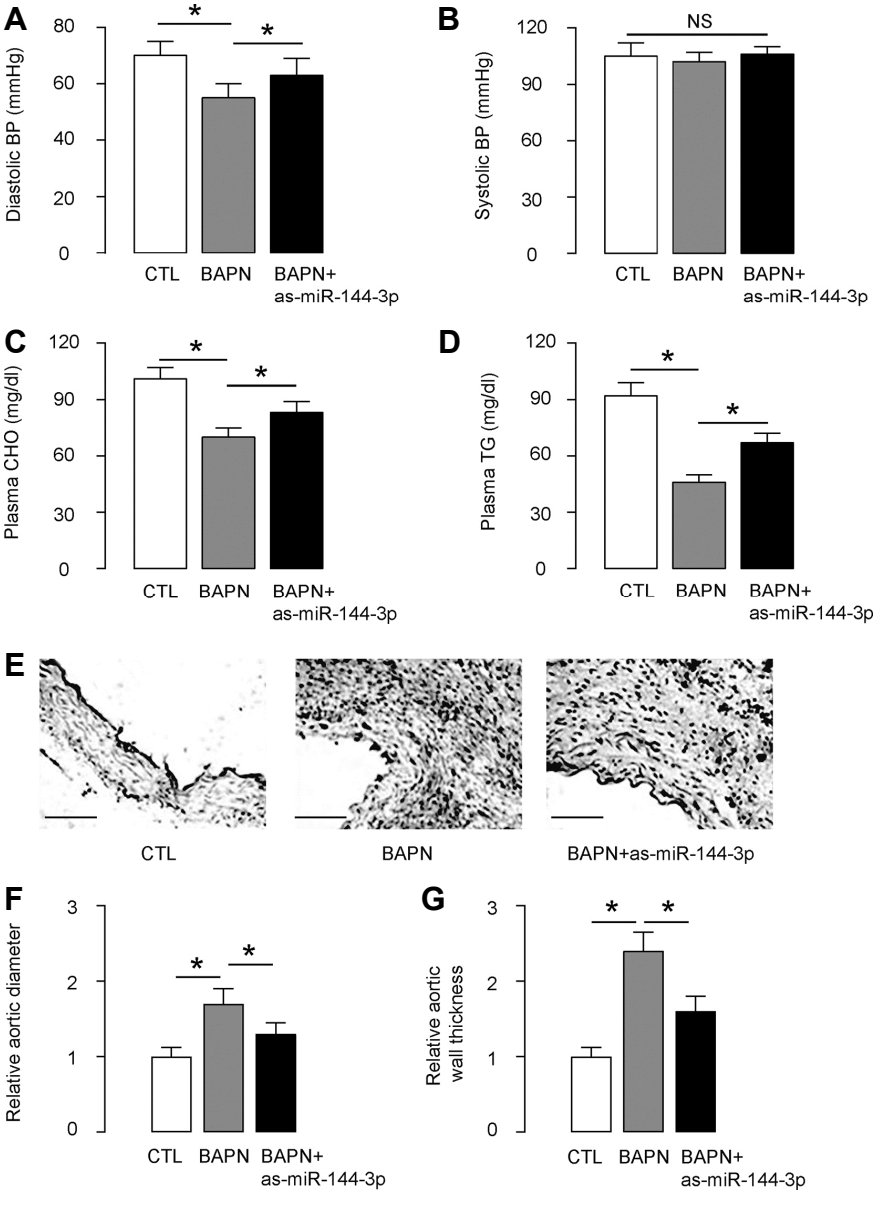

Fig. 5. Suppression of miR-144-3p reduces the incidence and severity of AD. A mouse model for AD was done. Ten mice were used in each experimental group. Three groups of mice were included in the study. In group 1, mice did not receive either BAPN or AAVs (CTL). In group 2, mice received BAPN and control AAV-null (BAPN). In group 3, mice received BAPN and AAV-as-miR-144-3p (BAPN+as-miR-144-3p). (A) Diastolic blood pressure (BP). (B) Systolic BP. (C) Plasma cholesterol (CHO). (D) Plasma triglyceride (TG). (E) Hematoxylin and eosin (H&E) staining in mouse aorta. (F) Aortic diameter. (G) Aortic wall thickness. $*p < 0.05$. NS: non-significant. N=10. Scale bars are 50 μm.

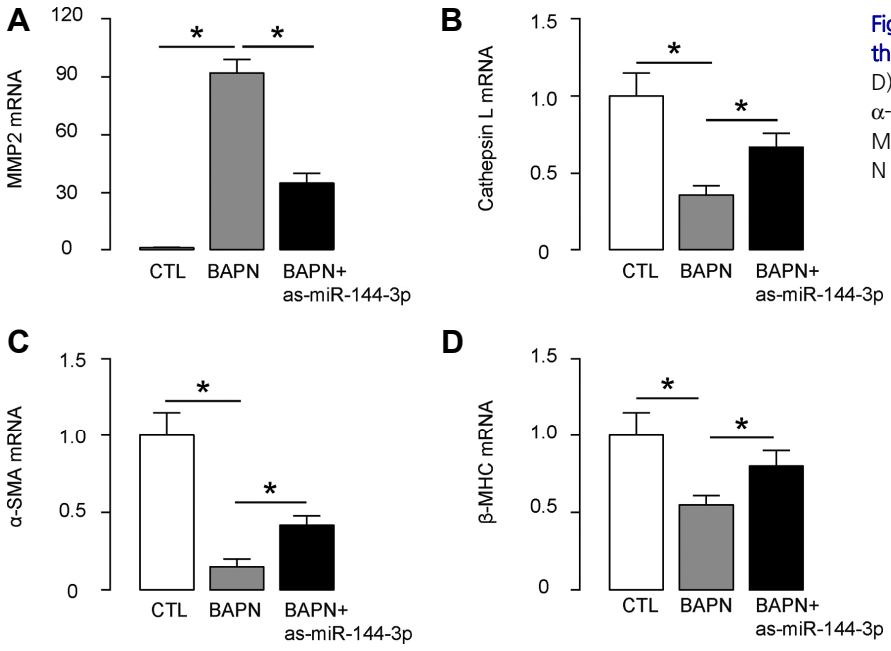

Fig. 6. Suppression of miR-144-3p reduced the expression of AD-associated genes. (A-D) RT-qPCR for MMP2 (A), Cathepsin L (B), α-SMA (C) and β-myosin heavy chain (β-MHC; D) in mouse aortic tissue. $*p < 0.05$. N = 10.

and triglyceride levels (Fig. 5D), which were both attenuated by miR-144-3p suppression (Figs. 5C and 5D). Furthermore, hematoxylin and eosin staining showed that the tearing of the aortic wall and thrombi in the false lumens in BAPN mice were also less severe in BAPN+as-miR-144-3p mice (Fig. 5E). BAPN treatment significantly increased aortic diameter (Fig. 5F) and aortic wall thickness (Fig. 5G), which were both attenuated by miR-144-3p suppression (Figs. 5F and 5G). Together, these data suggest that suppression of miR-144-3p reduces the incidence and severity of AD.

Suppression of miR-144-3p reduces the expression of AD-associated genes

Since BAPN-induced AD exhibited typical histological features of the human disease, we next examined the expression of AD-related genes in aortas. We found that BAPN-induced upregulation of MMP2, BAPN-induced downregulation of Cathepsin L, BAPN-induced downregulation of α-SMA and BAPN-induced downregulation of β-myosin heavy chain (β-MHC) were all attenuated by miR-144-3p suppression. These data provide a molecular mechanism underlying the miR-144-3p suppression induced reduction in the incidence and severity of AD in this model.

DISCUSSION

A lot of risk factors including hypertension, dyslipidaemia and genetic disorders may increase the chances of AD occurrence (Mallat et al., 2016). Progress in the understanding of the underlying pathophysiology of AD could lead to advances in the prognosis and prevention of AD in patients being considered at a substantial risk.

Previous studies have focused on the genetic predisposition to AD and the hereditary influence on AD onset (Mallat et al., 2016). However, as a focus of our AD study, TE-associated elastin durability appears to be critical for resisting AD (Mallat et al., 2016). Elastin is a major structural component of elastic fibers. Although the turnover of elastin appears to be extremely low, the continuous production and deposition seemed to be essential for ASMC to survive billions of cycles of stretch and recoil without mechanical failure (Helbig and Krzemien, 2004; Janoff, 1983; Nygaard et al., 2016; Stone et al., 1997). Major defects in the elastin/TE gene have been associated with supravalvular aortic stenosis, Williams-Beuren syndrome, autosomal dominant cutis laxa, as well as AD (Patel and Arora, 2008). However, to the best of our knowledge, this is the first study to show presence of post-transcriptional control of TE in ASMC that affects AD onset.

First, miR-144-3p was determined as a miRNA that functionally targets TE to reduce its protein translation in ASMC, which results in a negative influence on the TE production and secretion by ASMC. Interestingly, the presence of this regulatory axis in both HASMC and MASMC strengthened the power of this finding, as it may be highly possible to be extrapolated into clinical application. Next, in an established mouse model for AD, the suppression of miR-144-3p resulted in a reduction of AD occurrence ratio in weeks from 90% to 50%, which was supported by all features for AD examined in this study.

The regulatory axis of miR-144-3p/TE in smooth muscle cells here is not reported before. In 2008, it was reported that miR-29 family miRNAs are involved in the down-regulation of elastin in the adult aorta (Ott et al., 2011), and this regulation loop was further confirmed in some other models (Chuang et al., 2015; Ekman et al., 2013; Maegdefessel et al., 2012; Merk et al., 2012; Okamura et al., 2017; Sudo et al., 2015; Zhang et al., 2012). However, miR-

29 seemed to have a vast number of target genes, including MMP-2, a gene that altered highly in AD (Jiang et al., 2017). Hence, interpretation of miR-29 in AD onset should be very careful and many possible involved genes need to be examined. Compared to miR-29, miR-144-3p has much less confirmed target genes. Although E26 transformation specific-1 (Zhang et al., 2016), cyclooxygenase-2 (Shao et al., 2016), adenosine triphosphate binding cassette transporter (Vega-Badillo et al., 2016), and cyclin-dependent kinase inhibitor 2D (Jiang et al., 2015), have been reported as miR-144-3p-targeting genes, the involvement of these genes in the development of AD is very limited. Therefore, to reveal miR-144 as a TE-targeting miRNA and a highly expressing miRNA in ASMC is very important.

In the future, therapeutic effects of suppression of endogenous miR-144-3p in ASMC may be an attractive approach to treat patients with high AD risks, if the results from this work could be further confirmed and validated in human studies.

Note: Supplementary information is available on the Molecules and Cells website (www.molcells.org).

ACKNOWLEDGMENTS

This work was supported by the Special Fund for Science and Technology for Social Development in Hainan (No: 2015SF04).

REFERENCES

Agarwal, V., Bell, G.W., Nam, J.W., and Bartel, D.P. (2015). Predicting effective microRNA target sites in mammalian mRNAs. eLife *4*, doi: 10.7554/eLife.05005.

Cao, M.X., Jiang, Y.P., Tang, Y.L., and Liang, X.H. (2017). The crosstalk between lncRNA and microRNA in cancer metastasis: orchestrating the epithelial-mesenchymal plasticity. Oncotarget *8*, 12472-12483.

Chuang, T.D., Pearce, W.J., and Khorram, O. (2015). miR-29c induction contributes to downregulation of vascular extracellular matrix proteins by glucocorticoids. Am J Physiol Cell Physiol. *309*, C117-125.

Ekman, M., Bhattachariya, A., Dahan, D., Uvelius, B., Albinsson, S., and Sward, K. (2013). Mir-29 repression in bladder outlet obstruction contributes to matrix remodeling and altered stiffness. PLoS One *8*, e82308.

Forman, J.J., Legesse-Miller, A., and Coller, H.A. (2008). A search for conserved sequences in coding regions reveals that the let-7 microRNA targets Dicer within its coding sequence. Proc Natl Acad Sci U S A *105*, 14879-14884.

Helbig, G., and Krzemien, S. (2004). Clinical significance of elastin turnover--focus on diseases affecting elastic fibres. Wiad Lek *57*, 360-363.

Isselbacher, E.M., Lino Cardenas, C.L., and Lindsay, M.E. (2016). Hereditary Influence in Thoracic Aortic Aneurysm and Dissection. Circulation *133*, 2516-2528.

Ivey, K.N., Muth, A., Arnold, J., King, F.W., Yeh, R.F., Fish, J.E., Hsiao, E.C., Schwartz, R.J., Conklin, B.R., Bernstein, H.S., et al. (2008). MicroRNA regulation of cell lineages in mouse and human embryonic stem cells. Cell Stem Cell *2*, 219-229.

Janoff, A. (1983). Do neutrophils play a major role in elastin turnover of normal tissues? Am. Rev. Respir. Dis. *127*, 782-783.

Jiang, W., Zhang, Z., Yang, H., Lin, Q., Han, C., and Qin, X. (2017). The involvement of miR-29b-3p in arterial calcification by targeting matrix metalloproteinase-2. BioMed. Res. Int. *2017*, 6713606.

Jiang, X., Shan, A., Su, Y., Cheng, Y., Gu, W., Wang, W., Ning, G., and Cao, Y. (2015). miR-144/451 Promote cell proliferation via targeting PTEN/AKT pathway in insulinomas. Endocrinology *156*, 2429-2439.

Li, Q. and Gregory, R.I. (2008). MicroRNA regulation of stem cell fate. Cell Stem Cell *2*, 195-196.

Maegdefessel, L., Azuma, J., Toh, R., Merk, D.R., Deng, A., Chin, J.T., Raaz, U., Schoelmerich, A.M., Raiesdana, A., Leeper, N.J., et al. (2012). Inhibition of microRNA-29b reduces murine abdominal aortic aneurysm development. J. Clin. Invest. *122*, 497-506.

Mallat, Z., Tedgui, A., and Henrion, D. (2016). Role of microvascular tone and extracellular matrix contraction in the regulation of interstitial fluid: implications for aortic dissection. Arterioscler. Thromb. Vasc. Biol. *36*, 1742-1747.

Merk, D.R., Chin, J.T., Dake, B.A., Maegdefessel, L., Miller, M.O., Kimura, N., Tsao, P.S., Iosef, C., Berry, G.J., Mohr, F.W., et al. (2012). miR-29b participates in early aneurysm development in Marfan syndrome. Circ. Res. *110*, 312-324.

Morello, F., Piler, P., Novak, M., and Kruzliak, P. (2014). Biomarkers for diagnosis and prognostic stratification of aortic dissection: challenges and perspectives. Biomarkers Med. *8*, 931-941.

Nygaard, R.H., Maynard, S., Schjerling, P., Kjaer, M., Qvortrup, K., Bohr, V.A., Rasmussen, L.J., Jemec, G.B., and Heidenheim, M. (2016). Acquired localized cutis laxa due to increased elastin turnover. Case Rep. Dermatol. *8*, 42-51.

Okamura, H., Emrich, F., Trojan, J., Chiu, P., Dalal, A.R., Arakawa, M., Sato, T., Penov, K., Koyano, T., Pedroza, A., et al. (2017). Long-term miR-29b suppression reduces aneurysm formation in a Marfan mouse model. Physiol. Rep. *5*, pii: e13257.

Ott, C.E., Grunhagen, J., Jager, M., Horbelt, D., Schwill, S., Kallenbach, K., Guo, G., Manke, T., Knaus, P., Mundlos, S., et al. (2011). MicroRNAs differentially expressed in postnatal aortic development downregulate elastin via 3' UTR and coding-sequence binding sites. PLoS One *6*, e16250.

Papagiannakopoulos, T., and Kosik, K.S. (2009). MicroRNA-124: micromanager of neurogenesis. Cell Stem Cell *4*, 375-376.

Patel, P.D., and Arora, R.R. (2008). Pathophysiology, diagnosis, and management of aortic dissection. Ther Adv Cardiovasc Dis *2*, 439-468.

Ray, J.L., Leach, R., Herbert, J.M., and Benson, M. (2001). Isolation of vascular smooth muscle cells from a single murine aorta. Methods Cell Sci. *23*, 185-188.

Sato, F., Seino-Sudo, R., Okada, M., Sakai, H., Yumoto, T., and Wachi, H. (2017). Lysyl Oxidase Enhances the Deposition of Tropoelastin through the Catalysis of Tropoelastin Molecules on the Cell Surface. Biol. Pharm. Bull. *40*, 1646-1653.

Segreto, A., Chiusaroli, A., De Salvatore, S., and Bizzarri, F. (2014). Biomarkers for the diagnosis of aortic dissection. J. Card Surg. *29*, 507-511.

Seok, H., Ham, J., Jang, E.S., and Chi, S.W. (2016). MicroRNA target recognition: insights from transcriptome-wide non-canonical interactions. Mol. Cells *39*, 375-381.

Shao, Y., Li, P., Zhu, S.T., Yue, J.P., Ji, X.J., Ma, D., Wang, L., Wang, Y.J., Zong, Y., Wu, Y.D., et al. (2016). MiR-26a and miR-144 inhibit proliferation and metastasis of esophageal squamous cell cancer by inhibiting cyclooxygenase-2. Oncotarget *7*, 15173-15186.

Stone, P.J., Lucey, E.C., Snider, G.L., and Franzblau, C. (1997). Distribution of elastin in hamsters and the turnover rates of different elastin pools. Proc. Soc. Exp. Biol. Med. *215*, 94-101.

Sudo, R., Sato, F., Azechi, T., and Wachi, H. (2015). MiR-29-mediated elastin down-regulation contributes to inorganic phosphorus-induced osteoblastic differentiation in vascular smooth muscle cells. Genes Cells *20*, 1077-1087.

Vega-Badillo, J., Gutierrez-Vidal, R., Hernandez-Perez, H.A., Villamil-Ramirez, H., Leon-Mimila, P., Sanchez-Munoz, F., Moran-Ramos, S., Larrieta-Carrasco, E., Fernandez-Silva, I., Mendez-Sanchez, N., et al. (2016). Hepatic miR-33a/miR-144 and their target gene ABCA1 are associated with steatohepatitis in morbidly obese subjects. Liver Int. *36*, 1383-1391.

Zhang, P., Huang, A., Ferruzzi, J., Mecham, R.P., Starcher, B.C., Tellides, G., Humphrey, J.D., Giordano, F.J., Niklason, L.E., and Sessa, W.C. (2012). Inhibition of microRNA-29 enhances elastin levels in cells haploinsufficient for elastin and in bioengineered vessels--brief report. Arterioscler Thromb. Vasc. Biol. *32*, 756-759.

Zhang, S.Y., Lu, Z.M., Lin, Y.F., Chen, L.S., Luo, X.N., Song, X.H., Chen, S.H., and Wu, Y.L. (2016). miR-144-3p, a tumor suppressive microRNA targeting ETS-1 in laryngeal squamous cell carcinoma. Oncotarget *7*, 11637-11650.